ERDC/EL MP-20-8

US Army Corps
of Engineers®
Engineer Research and
Development Center

Removing Uranium (VI) from Aqueous Solution With Insoluble Humic Acid Derived from Leonardite

Fande Meng, Guodong Yuan, Steven L. Larson, John H. Ballard,
Charles A. Waggoner, Zikri Arslan, and Fengxiang X. Han

July 2020

Environmental Laboratory

The U.S. Army Engineer Research and Development Center (ERDC) solves the nation's toughest engineering and environmental challenges. ERDC develops innovative solutions in civil and military engineering, geospatial sciences, water resources, and environmental sciences for the Army, the Department of Defense, civilian agencies, and our nation's public good. Find out more at www.erdc.usace.army.mil.

To search for other technical reports published by ERDC, visit the ERDC online library at http://acwc.sdp.sirsi.net/client/default.

ERDC/EL MP-20-8
July 2020

Removing Uranium (VI) from Aqueous Solution With Insoluble Humic Acid Derived from Leonardite

Steven L. Larson and John H. Ballard

Environmental Laboratory
U.S. Army Engineer Research and Development Center
3909 Halls Ferry Road
Vicksburg, MS 39180

Fande Meng, Zikri Arslan, and Fengxiang X. Han

Department of Chemistry and Biochemistry
Jackson State University
Jackson, MS 39217

Guodong Yuan

Zhaoqing University
Zhaoqing, Guangdong 526061, China

Charles A. Waggoner

Institute for Clean Energy Technology
Mississippi State University
Starkville, MS 39759

Final report

Prepared for U.S. Army Corps of Engineers
Washington, DC 20314

Under Project Number 458170, “Depleted Uranium (DU) Clearance from DoD Ranges”

Abstract

The occurrence of uranium (U) and depleted uranium (DU)-contaminated wastes from anthropogenic activities is an important environmental problem. Insoluble humic acid derived from leonardite (L-HA) was investigated as a potential adsorbent for immobilizing U in the environment. The effect of initial pH, contact time, U concentration, and temperature on U(VI) adsorption onto L-HA was assessed. The U(VI) adsorption was pH-dependent and achieved equilibrium in 2 h. It could be well described with pseudo-second- order model, indicating that U(VI) adsorption onto L-HA involved chemisorption. The U(VI) adsorption mass increased with increasing temperature with maximum adsorption capacities of 91, 112 and 120 mg g^{-1} at 298, 308 and 318 K, respectively. The adsorption reaction was spontaneous and endothermic. We explored the processes of U(VI) desorption from the L-HA-U complex through batch desorption experiments in 1 mM NaNO3 and in artificial seawater. The desorption process could be well described by pseudo-first-order model and reached equilibrium in 3 h. L-HA possessed a high propensity to adsorb U(VI). Once adsorbed, the release of U(VI) from L-HA-U complex was minimal in both 1 mM $NaNO_3$ and artificial seawater (0.06% and 0.40%, respectively). Being abundant, inexpensive, and safe, LHA has good potential for use as a U adsorbent from aqueous solution or immobilizing U in soils.

Preface

This study was conducted for the U.S. Army Corps of Engineers under Project 458170, titled, "Depleted Uranium (DU) Clearance from DoD Ranges." The Grant Officer's Technical Representative was Mr. John H. Ballard, Office of the Technical Director for Installations and Operational Environments, ERDC-EL-EZT and the Technical Point of Contact was Dr. Steven L. Larson, Environmental Engineering Branch, ERDC-EL-EPE.

The work was performed by the Environmental Engineering Branch of the Environmental Processes Division, U.S. Army Engineer Research and Development Center, Environmental Laboratory (ERDC-EL). At the time of publication of this Miscellaneous Paper, Ms. Brooke Petery was Acting Branch Chief; Dr. Brandon Lafferty was Acting Division Chief; and Dr. Elizabeth Ferguson was the Technical Director for Installations and Operational Environments. The Acting Deputy Director of ERDC-EL was Dr. Justin Berman and the Acting Director was Dr. Jack Davis.

This report documents a collaborative study conducted under the sponsorship of the U.S. Army Futures Command with FY18 Congressional Program Increase Funds in PE 0603728A in the Fiscal Year (FY) 2018 Department of Defense Appropriations Act. Collaborative work was conducted by the U.S. Army Engineer Research and Development Center and Jackson State University via Cooperative Agreement W912HZ-16-2-0021.

The Commander of ERDC was COL Teresa A. Schlosser and the Director was Dr. David W. Pittman.

Removing uranium (VI) from aqueous solution with insoluble humic acid derived from leonardite

1. Introduction

Uranium (U) occurs naturally in several minerals as a mixture of three isotopes, U-238, U-235, and U-234 (Cordfunke, 1970). Depleted uranium (DU) is a by-product of the production of enriched uranium containing U-235 and U-234 at lower concentrations than natural U (AEPI, 1995). DU is used in kinetic energy penetrators and armor plating as well as having widespread applications as aircraft counterweights and radiation shielding in medical radiation therapy (Betti, 2003; Global Security, 2008). Leaching of U to water occurs naturally due to interaction with soil minerals (Choy et al., 2006; Munasinghe et al., 2015). Anthropogenic contamination also arises from U ore mining/processing, medical waste, nuclear power station operation, accidents, and weapons testing. Acid drainage water from U mine tailings contains U and other radionuclides at low pH, reported from sites worldwide, including Australia (Mudd and Patterson, 2010), Germany (Biehler and Falck, 1999), Canada (Berthelot et al., 1999), and Brazil (Campos et al., 2011). This has resulted in the release of U-and DU-containing wastes into soil and groundwater environments, posing risks to surface water and human health (Lienert et al., 1994; Krestou et al., 2004; Todorov and Ilieva, 2006; Gavrilescu et al., 2009; Steinhauser et al., 2014). U usually occurs as U^{6+} and U^{4+} oxidation states in soil and water environments and U^{6+} is the main stable valence under oxidizing conditions. The daily intake of U, as established by the World Health Organization (WHO), is 0.6 μg kg^{-1} of body weight/day; the maximum U concentration in drinking water at 15 μg L^{-1} (WHO, 2008) or30 μg/L (U.S. Environmental Protection Agency, 2012).

A range of technologies have been developed for removing U from water, including adsorption, membrane processes, chemical precipitation, and ion-exchange (Dulama et al., 2013). Adsorption has become a popular choice due to its cost-effectiveness and ease of operation. Adsorbents used to remove U from water, include microbial biomass (Kalin et al., 2004), activated carbon (Mellah et al., 2006), hematite (Xie et al., 2009), sepiolite (Donat, 2009), clay materials (Campos et al., 2013) and clay-humic complexes (Anirudhan et al., 2010). Recently, biopolymers, such as insoluble humic acids (HA), have been extensively used as adsorbents of heavy metals (Havelcová et al., 2009; Shaker and Albishri, 2014; Khalili and Al-Banna, 2015; Meng et al., 2016). HAs are naturally occurring in water and soil environments and play a vital role in environmental detoxification (Kochany and Smith, 2001; Yuan and Theng, 2012; Ziółkowska, 2015). They could also be extracted from leonardite and lignite. With abundant functional groups (e.g., quinone, amino, carboxylic, phenolic), leonardite-derived HA (L-HA) has a good propensity to bind metal cations (Olivella et al., 2002; Yang et al., 2015).

The objective of this work was to investigate the potential use of L-HA as a U adsorbent from U waste water such as mining tailing as well as other U contaminated sites such as army shooting ranges. To this end, the effects of pH, contact time, temperature, and initial U(VI) concentrations on U adsorption were assessed through kinetics adsorption experiments at 298 K and batch isotherm experiments at 298, 308 and 318 K. Further, the process of U(VI) desorption from the L-HA-U complex was investigated with batch kinetics desorption experiments at 298 K. Desorption studies were performed using diluted $NaNO_3$ as a background electrolyte to simulate a normal soil solution (Harter and Naidu, 2001) and artificial seawater as a marine environment simulant to study the tendency of U(VI) release from L-HA-U complex.

2. Experimental

2.1. Materials, reagents and preparation of solutions

Leonardite was purchased from Xinjiang Uyghur Autonomous Region, China, which was similar in physical and chemical properties to leonardite from North Dakota, US. All reagents used in this study were of analytical grade. Nitric acid and sodium hydroxide, used for adjusting pH, were purchased from Thermo Fisher. Uranyl nitrate, 1% aqueous, was purchased from Poly Scientific R&D Corp. A series of U(VI) solutions were prepared by successively diluting the uranyl nitrate 1% aqueous with 1 mM $NaNO_3$. A single element standard for U was obtained from SPEX CertiPrep and used to prepare standard curves for quantitation. Artificial seawater was prepared according to the methods of Yu et al. (2011) and consisted of 26.5 g/L NaCl + 24 g/L $MgCl_2$ + 0.73 g/L KCl + 3.3 g/L $MgSO_4$ + 0.2 g/L $NaHCO_3$ + 1.1 g/L $CaCl_2$ + 0.28 g/L NaBr.

2.2. Preparation and characterization of L-HA

The traditional alkaline-acid procedure was used to obtain HA from leonardite (Havelcová et al., 2009; Meng et al., 2016). Briefly, 50 g leonardite were added to 500 mL of 0.1 M NaOH solution in a Teflon-lined container, heated to 40 °C, then sonicated for 30 min. After standing overnight in the sealed container, the supernatant liquid was slowly poured off and 0.1 M NaOH was added to the solid residue. This extraction procedure was repeated six times. The L-HA was obtained by adding 6 M HCl to the collected supernatant liquid while stirring to pH 2, centrifuging at 3000 r•min^{-1} for 15 min and washing the precipitate with deionized water, and centrifuging for three times. The final precipitation with pH 4.02 was freeze-dried for use.

The L-HA was analyzed for its physical and chemical properties. Ash content of the L-HA was determined by heating samples in a muffle furnace at 800 °C for 4 h under air atmosphere. Elemental contents were determined by an elemental analyzer (Vario micro cube, Elementar, Germany) for dried sample. The pH was determined in boiled, distilled water with a pH meter at a solid-liquid ratio of 1: 10 (Mettler Toledo, Switzerland). Surface morphology was observed with a Scanning Electron Microscope (SEM, Hitachi S-4800, Japan, 3 kV). Functional groups were analyzed with Fourier transform infrared spectroscopy (Thermo Nicolet, 470 FTIR, USA). Acidic functional groups were quantified according to the method of International Humic Substances Society (http://www.humicsubstances.org/acidity.html). Briefly, a solution containing 0.36 ± 0.01 g L^{-1} (base on a dry ash-free) of HA (with pH adjusted to 3.0 with HCl and 0.1 M NaCl as background electrolyte) was titrated with carbonate-free 0.1 M NaOH at 25 °C to pH 8.0 and 10.0. The contents of carboxyl and phenolic-OH groups were calculated from NaOH consumption between pH 3.0 and 8.0 and between 8.0 and 10.0, respectively.

2.3. Batch experiments

2.3.1. Batch adsorption experiments

First, initial U solutions (60 mg/L) were prepared. The pH values of the U solutions were adjusted to pH 3, 4, 5, 6, 7, 8 with 0.1 M HNO_3 or NaOH solutions before mixing with L-HA. Dissolved U in pH adjusted solutions was measured again. Twenty mg (accurate to 0.0001 g) L-HA was added to 50 mL centrifuge tubes containing 30 mL U solution. The tubes were capped and placed on a temperature controlled shaker at 298 K. After 12 h of shaking the tubes were centrifuged, and the supernatants filtered through 0.45-μm membrane (Whatman, UK). The clear supernatants were diluted with 1% HNO_3 for U analysis with a Varian 820-ICP-MS, (Varian Inc., USA) where the U concentrations should be less than 100 μg/L. The kinetic study was conducted in the solution with pH 5.0 at 298 K for 0.1, 0.25, 0.5, 0.75, 1, 1.5, 2, 3, and 4 h. The initial U concentrations are high for most U contaminated sites, however, this research effort is partially directed toward military shooting ranges, where U concentrations in soil have been reported as high as 2700 mg/kg (Larson et al., 2009). To simulate high concentrations of absorbed U in a solid matrix, a relatively high initial U concentration such as those used in the present study seemed desirable.

Adsorption thermodynamics were assessed with initial U(VI) concentrations from 5 to 120 mg L^{-1} at three temperatures (298, 308 and 318 K). Thirty mL of the U(VI) solutions were added into 50 mL centrifuge tubes containing 20 mg L-HA. The initial pH of U(VI) solution was adjusted to 5 ± 0.05 and shaken for 12 h.

2.3.2. Batch desorption experiments

A L-HA-U complex was prepared for the desorption experiments by adding 1 g L-HA to a PTEE bottle with 250 mL of 120 mg L^{-1} of U solution. The initial pH was adjusted to 5.0 ± 0.1 using HNO_3 or NaOH. After shaking for 12 h at 298 K, the bottle was centrifuged and the obtained residue (L-HA-U complex) was dried at 105 °C until constant weight.

Desorption of the U(VI) from the L-HA matrix was studied using 1 mM $NaNO_3$ (as a simulated soil solution) (Harter and Naidu, 2001) or artificial seawater. Twenty mg of the L-HA-U were placed into 50 mL tubes containing 30 mL of a 1 mM $NaNO_3$ solution with a pH 5.03, or artificial seawater with a pH 6.98. The tubes were capped and continuously shaken in a temperature controlled shaker at 298 K. The shaking time are 0.25, 0.5, 0.75, 1, 1.5, 2, 3 and 4 h for artificial seawater, and 0.25, 0.5, 0.75, 1, 1.5, 2, 3, 4, 6 and 8 h for 1 mM $NaNO_3$. The supernatants were filtered and analyzed for U concentration by ICP-MS.

All batch adsorption and desorption experiments were performed in duplicates.

The adsorption or desorption mass was calculated by the differences of U concentration in solution before and after adsorption or desorption. Software Origin8.0 (OriginLab. USA) was used for data processing.

2.4. Models

2.4.1. Adsorption and desorption kinetics models

The pseudo-first-order model and pseudo-second-order model are often used to describe adsorption or desorption dynamics processes.

The pseudo-first-order model equation (Eq. (1)) describes adsorption in solid-liquid system on the basis of adsorption capacity of solid (Ho, 2004),

$$q_t = q_1\left(1 - e^{-k_1 t}\right) \tag{1}$$

The pseudo-second-order model equation (Eq. (2)) has been applied for analyzing the mechanism of adsorption processes involving chemisorption from liquid solution (Ho and McKay, 1999; Ho, 2006),

$$q_t = \frac{q_2^2 k_2 t}{1 + q_2 k_2 t} \tag{2}$$

where q_1 and q_2 are the amount of U(VI) sorbate onto or desorbed from adsorbent at the equilibrium state ($mg{\bullet}g^{-1}$), q_t is the amount of sorbate adsorbed onto or desorbed from adsorbent at time t ($mg{\bullet}g^{-1}$), k_1 is the pseudo-first-order equilibrium rate constant ($1{\bullet}h^{-1}$), and k_2 is the pseudo-second-order equilibrium rate constant ($g{\bullet}(mg{\bullet}h)^{-1}$).

2.4.2. Adsorption isotherms models

An adsorption isotherm model can be used to describe the adsorption between liquid and solid phases at equilibrium state. The adsorption of U(VI) by L-HA was modelled using the Langmuir and Freundlich models. The Langmuir model assumes a uniform monolayer adsorption, while the Freundlich model is based on heterogeneous adsorption not restricted by monolayer (Yang, 1998; Mellah et al., 2006). The Langmuir and Freundlich models equations are as follows.

Langmuir equation,

$$q = \frac{q_m k_L C_e}{1 + k_L C_e} \tag{3}$$

Freundlich equation,

$$q = k_F C_e^{1/n} \tag{4}$$

where C_e is the equilibrium concentration ($mg{\bullet}L^{-1}$), q is the amount of U(VI) adsorbed onto L-HA at equilibrium state ($mg{\bullet}g^{-1}$), q_m is the maximum capacity for U(VI) ($mg{\bullet}g^{-1}$), k_L is a constant related to the affinity of the binding sites ($L{\bullet}mg^{-1}$), k_F is the equilibrium adsorption constant related to adsorption capacity ($mg^{(1-n)}{\bullet}L^n{\bullet}g^{-1}$), and 1/n is a constant related to adsorption intensity.

2.4.3. Thermodynamic parameters

The thermodynamic parameters were determined from the thermodynamic equilibrium constant, K_0. The standard Gibbs free energy $\triangle G^0$ ($kJ{\bullet}mol^{-1}$), standard enthalpy change $\triangle H^0$ ($kJ{\bullet}mol^{-1}$), and standard entropy change $\triangle S^0$ ($J{\bullet}(mol{\bullet}K)^{-1}$) were calculated using the following equations,

$$\triangle G^0 = -RT\ln K_0 \tag{5}$$

$$\ln K_0 = \frac{\triangle S^0}{R} - \frac{\triangle H^0}{RT} \tag{6}$$

and K_0 can be defined as the following equation where:

$$K_0 = \frac{q_e}{C_e} \tag{7}$$

where R is the gas constant ($8.314\ J{\bullet}(mol{\bullet}K)^{-1}$), T is the temperature in K, C_e is the equilibrium concentration ($mmol{\bullet}L^{-1}$), and q_e is the amount of U(VI) adsorbed on L-HA at equilibrium state ($mmol{\bullet}g^{-1}$).

3. Results and discussion

3.1. Properties of HA

The L-HA had a pH value of 4.02, an ash content of 7.87%, and carbon content of 58.7%. The size and shape of the L-HA precipitate particles may greatly impact adsorption rate and capacity. SEM graphics of fresh L-HA indicated that its surface was heterogeneous and fully covered by small spherical particles (Fig. 1). As a sphere has the largest surface area for a given volume, the small spherical particles would favor U adsorption onto the L-HA surface. According to Stevenson (1994) and Tan (2014), the spectra of L-HA showed oxygen-containing functional groups which appear at about 3414 cm^{-1} (O-H stretching of H-bonded hydroxyl group and partially N-H stretch), 1700 cm^{-1} (C=O stretch of COOH), 1570 and 1353 cm^{-1} (anti-symmetrical and symmetrical stretching of COO−), and 1190 cm^{-1} (C-O stretch or phenolic C-OH) (Fig. 2). The carboxyl and phenolic-OH functional groups of L-HA were 6.18 and 1.82 moL/kg C, respectively. Soler-Rovira et al. (2010) observed a strong correlation between the carboxyl group content of HA and its adsorption capacity for heavy metals. Thus, the L-HA used in this study would have a high adsorption capacity for metal cations.

3.2. Effect of initial pH

Matrix pH is an important factor controlling the adsorption process of U(VI) onto L-HA because it may influence the surface charge of L-HA and change the U speciation in solution as well as solubility of humic substances (Misaelides et al., 1995; Camacho et al., 2010; Khalili and Al-Banna, 2015). As shown in Fig. 3, U(VI) adsorption onto L-HA was pH-dependent and the maximum U adsorption occurred at pH 6.0. At low pH the positive charge arising from amino groups on the surface of L-HA increases, which increases the competition of H^+ for U at surface binding sites and reduces the U adsorption (Wang et al., 2010). At pH < 3.0, UO_2^{2+} is the dominant species for adsorption; at pH 3.0−5.0, $(UO_2)_2(OH)_2^{2+}$, $(UO_2)_3(OH)_4^{2+}$ and $(UO_2)_3(OH)_5^{+}$ are present for adsorption; at pH > 5.0, intense hydrolysate ($(UO_2)_4(OH)_7^{+}$) occurred and were adsorbed (Misaelides et al., 1995; Camacho et al., 2010). The ionization of L-HA increases with pH, resulting in an increase in negative charge that allows adsorption of more mass of U. The resolubilization of L-HA below pH 6 was tested and found to be low (<0.20%), becoming negligible (<0.10%) in the presence of U. However, resolubilization of L-HA increased above pH 6.0. Some precipitate in U solution was observed at pH 8 before mixing with L-HA. Thus, at pH > 6.0, the dissolution of L-HA complexes, as well as the formation of U(VI) hydroxide species (e.g., $UO_2(OH)_2$), reduced U(VI) adsorption onto the L-HA (Camacho et al., 2010;

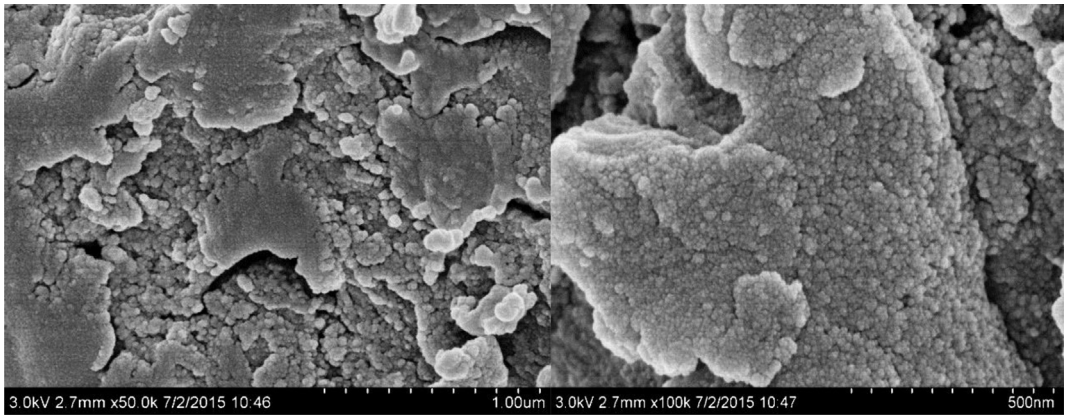

Fig. 1. SEM graphs of fresh L-HA particles.

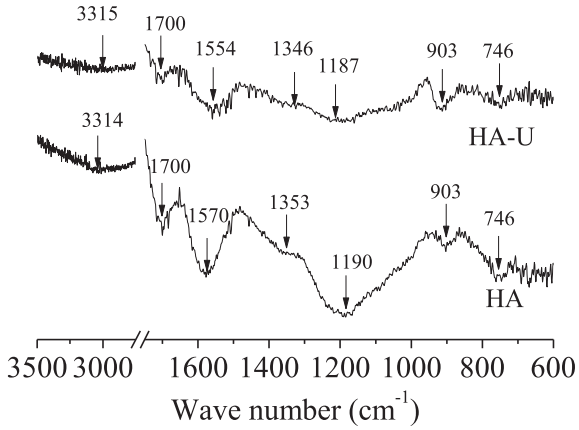

Fig. 2. FTIR spectra of L-HA and HA-U.

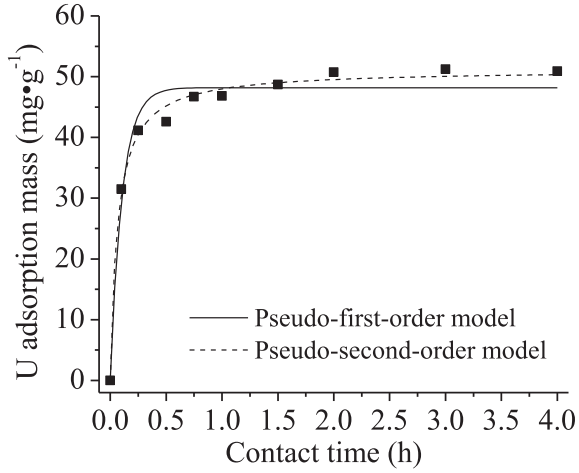

Fig. 3. Effect of pH on the adsorption mass of U(VI) by L-HA. The pH values of U solution (initial U 60 mg/L) were adjusted to pH 3, 4, 5, 6, 7, 8 before mixing with L-HA. Dissolved U in pH adjusted solutions was measured.

Wang et al., 2010; Milja et al., 2011). The mass of U adsorbed at pH 5.0 was 60 mg•g^{-1}and increased to 67 mg g^{-1} at pH 6.0. Since U-contaminated water, such as uranium mining wastewater, is usually an acidic condition, we selected pH 5 for kinetics and thermodynamic adsorption experiments to better simulate that environment.

3.3. Adsorption kinetics

Reaction time is another important factor influencing U(VI) adsorption onto L-HA (Fig. 4). Pseudo-first-and second-order models are often used to describe adsorption or desorption dynamic processes. U adsorption mass increased quickly in the initial 0.25 h and then increased slowly until an equilibrium state was reached at 2 h. In order to describe the adsorption process and explore the adsorption mechanism, the adsorption data obtained at 298 K were fitted to pseudo-first-order and pseudo-second-order models.

The values of adsorption kinetic parameters and coefficients of determination (R^2) from the models were summarized in Table 1. Both pseudo first and second models gave good R^2 values. The pseudo-second-order model yielded a slightly higher R^2 value (which was close to 1) and close agreement between adsorption mass value (q_2) and the experimental q_e. This suggests that U(VI) adsorption onto L-HA involves chemisorption, such as ion-exchange, chelation and surface-complexation (Ho and McKay, 1999; Ho, 2006).

3.4. Adsorption isotherm

Fig. 5 demonstrates that U adsorption increased with rising initial concentrations and temperature. In order to quantify the potential adsorption capacities of L-HA for U(VI) at different temperatures, the data obtained from batch experiments was fitted

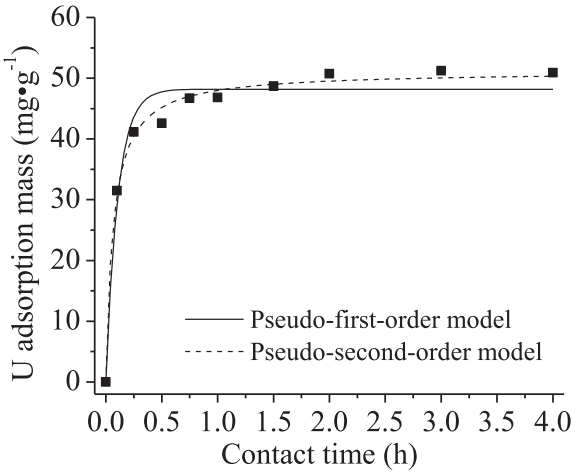

Fig. 4. Kinetics of U(VI) adsorption onto L-HA.

Table 1
Parameters of kinetic models for U(VI) adsorption onto L-HA.

q_e (mg•g^{-1})	Pseudo-first-order			Pseudo-second-order		
	q_1 (mg•g^{-1})	k_1 (1•h^{-1})	R^2	q_2 (mg•g^{-1})	k_2 (g• (mg•h)$^{-1}$)	R^2
51.2	48.2	9.42	0.97	51.2	0.29	0.99

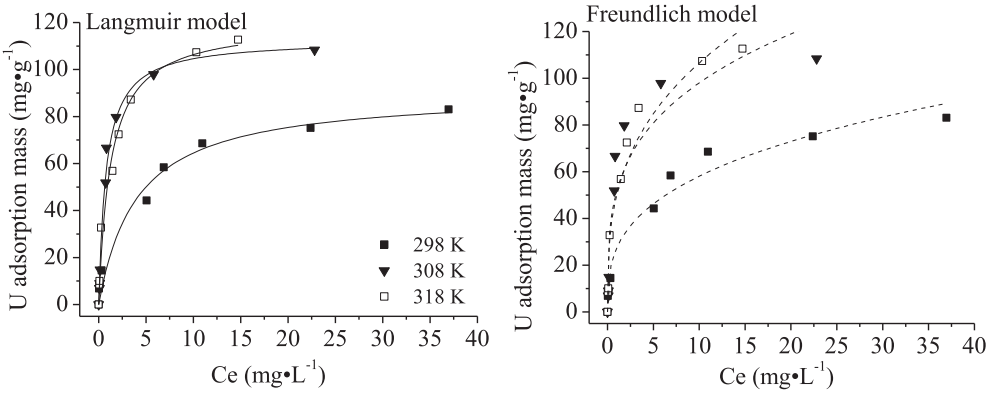

Fig. 5. Isotherms of U(VI) adsorption onto L-HA. (a) Langmuir model; (b) Freundlich model.

using the Langmuir model (Eq. (3)) and Freundlich model (Eq. (4)).

In general, as temperature increased, the ionization of carboxylic acids also increased, making the surface of adsorbents more reactive towards adsorption (Ellis, 1963; Uslu and Tanyol, 2006). The adsorption capacity of U(VI), calculated using the Langmuir model, increased from 91 mg g^{-1} at 298 K to 112 mg g^{-1} at 308 K, and then to 120 mg g^{-1} at 318 K, which were higher than other organic materials, such as cross-linked chitosan (Wang et al., 2009) and activated carbon (Kütahyalı and Eral, 2010). The adsorption data were well fitted to the Freundlich and Langmuir models (Table 2), however, the Langmuir model seemed more suitable than Freundlich model ($R_L^2 > R_F^2$) at experimental temperatures. This may be a result of surface and collision energy change with temperature (Van den Boomgaard et al., 1978; Michelsen et al., 1992; Uslu and Tanyol, 2006). Rising temperature increases surface activity of adsorbents and the kinetic energy of U, thus increasing the potential for its adsorption. The Langmuir model has been extensively used to describe the adsorption processes of heavy metals, even reactions with low reversibility, indicating a strong affinity and binding (Lasheen et al., 2012). The k_L is the adsorption equilibrium constant indicating the affinity of binding sites. The k_L increased and then decreased with increasing temperature, implying that the affinity of binding sites changed with temperature. This might not necessarily be related to changes in the dominant adsorption mechanism in a specific temperature range (Uslu and Tanyol, 2006).

3.5. Desorption experiments

The L-HA-U complex for desorption experiments contained 30.84 mg U/g. Desorption experiments were investigated with 1 mM $NaNO_3$ to simulate a soil-water system and artificial seawater to simulate a marine environment.

3.5.1. Uranium desorption in 1 mM $NaNO_3$

U desorption from L-HA-U in 1 mM $NaNO_3$, a soil simulant, increased quickly as time increased from 0.25 to 2 h and then reached an apparent equilibrium at 3 h (Fig. 6a). Desorption processes took a longer time to reach equilibrium than adsorption processes. At equilibrium, the desorption mass of U(VI) was 19 μg g^{-1} (only 0.06% of the adsorbed mass), indicating that the L-HA had a high retention capacity for U(VI), and thus good potential use as an inexpensive adsorbent in uranium contaminated soil.

3.5.2. Uranium desorption in artificial seawater

U(VI) desorption in artificial seawater increased quickly as time increased from 0.25 to 1.5 h and then slowly increased to reach an equilibrium at 3 h (Fig. 6b). The equilibrium desorption mass (q_e) of U(VI) was 125 μg g^{-1}, 0.4% of the adsorbed mass. This was higher than that in 1 mM $NaNO_3$, which is in agreement with results in literature (Ladshaw et al., 2015) and could be explained by three potential mechanisms: 1) seawater with high ionic strength contains cations (e.g., Mg^{2+}, Ca^{2+}) that compete with U(VI) adsorption onto L-HA (Anagnostopoulos et al., 2017); 2) seawater has a pH > 6, which partially dissolves the L-HA releasing U back into solution; 3) CO_3^{2-} and HCO_3^- in seawater ($HCO_{3(aq)}^- + OH_{(aq)}^- \rightleftharpoons CO_{3(aq)}^{2-} + H_2O_{(l)}$) may easily form complexes with U (Krestou and Panias, 2004; Santos and Ladeira, 2011), thus competing with L-HA for U. In most U-contaminated seawater, the U concentration may not be as high as in this experiment. Meinrath et al. (2003) reported groundwater concentrations as high as 50 mg L^{-1} up to percent concentrations. Toque et al. (2014) found corrosion rates of

Table 2
Parameters of adsorption isotherms for U(VI) adsorption onto L-HA at different temperatures.

Temperature (K)	Freundlich model			Langmuir model		
	1/n	k_F (mg$^{(1-n)}$•L^n•g^{-1})	R^2	q_m (mg•g^{-1})	k_L (L•mg^{-1})	R^2
298	0.33	27.2	0.97	91	0.25	0.98
308	0.28	51.6	0.83	112	1.28	0.99
318	0.33	49.8	0.96	120	0.78	0.98

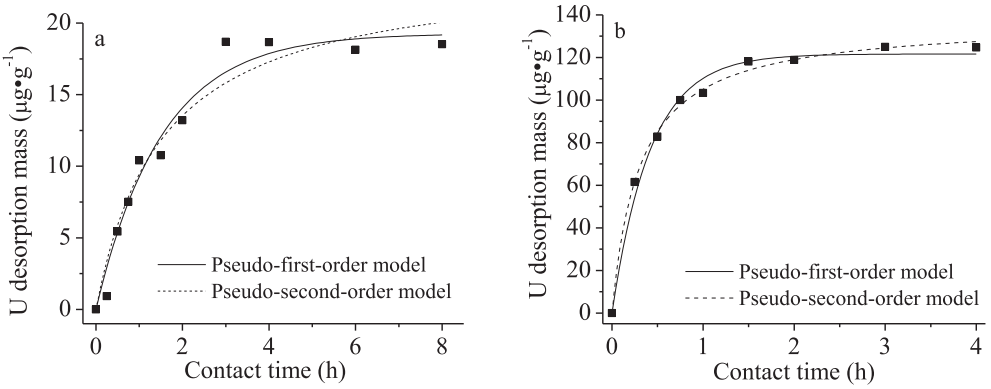

Fig. 6. Kinetics of U(VI) desorption from L-HA in: (a) 1 mM $NaNO_3$, (b) Artificial seawater.

1.9 g cm^{-2} y^{-1} from DU kinetic penetrator materials in the open ocean. Use of DU kinetic penetrators around marine environments might be expected to result in high uranium concentrations. The present finding indicates that the high retention capacity of L-HA for U(VI) could potentially be used to remove U(VI) from contaminated seawater.

3.5.3. Desorption kinetics

The U desorption processes could be described by the pseudo-first-order and pseudo-second-order models (Konvalinka et al., 1977; Tsai et al., 2008). Fitting parameters are displayed in Table 3. Although both equations fit the data well ($R^2 > 0.95$), q_1 was closer to q_e than q_2. This suggests that a pseudo-first-order model is more suitable than a pseudo-second-order model to describe the desorption process. This implies that desorption may be controlled by the abundance of adsorbed U on the surface of humic substances. Following an instantaneous release of adsorbed U at initial phase was a slow desorption with decreasing in the abundance of U on the surface. The initial fast desorption was due to U release from the external sorption sites of L-HA, whereas the slow desorption was due to diffusion-limited release of U from the internal sorption sites (McKinley et al., 2004; Tsai et al., 2008).

3.6. Adsorption thermodynamics

U(VI) adsorption (q_m) and $\ln K_0$ increased with rising temperature (Tables 2 and 4), suggesting that the adsorption process was endothermic (Boparai et al., 2011). This relationship implies that an increase in temperature favor U adsorption capacity with endothermic adsorption process.

Thermodynamic parameters for U(VI) adsorption onto L-HA were calculated using the measured data in Fig. 7a shows, the values of $\ln K_0$ at different temperatures were calculated from the plot of ln (q_e/C_e) versus q_e and supposing qe approach to zero (Fig. 7a) (Boparai et al., 2011; Khalili and Al-Banna, 2015). The values of $\ln K_0$ and $\triangle G^0$ calculated by equation (5) are summarized in Table 4. Negative values of $\triangle G^0$ indicate that the adsorption reaction was spontaneous and the extent of spontaneity of adsorption reaction increased with increasing temperature.

Table 4
Thermodynamic parameters for adsorption of U(VI) onto L-HA particles.

Temperature (K)	$\ln K_0$	$\triangle G^0$ (kJ•mol^{-1})
298	4.72	−11.7
308	4.91	−12.6
318	5.29	−14.0

According to equation (6), the values of $\triangle H^0$ and $\triangle S^0$ were determined by a plot of $\ln K_0$ versus 1/T (Fig. 6b) (Raji and Anirudhan, 1998; Boparai et al., 2011). The positive value of $\triangle S^0$ (115 J• (mol•K)$^{-1}$) revealed that the adsorption process was spontaneous and the affinity of L-HA for U(VI) was high for this system (Khalili and Al-Banna, 2015). The positive value of $\triangle H^0$ (22.5 kJ mol^{-1}) observed in this study indicates that the adsorption of U(VI) onto L-HA is endothermic, which is supported by the increasing U adsorption mass with increasing temperature. Due to limited kinetic experimental data at only one temperature, activation energy of DU adsorption process was not able to calculate. Thus, the detailed thermodynamic analyses of U adsorption was limited by current study.

3.7. Adsorption mechanism

L-HA had a complex structure, with high content of functional groups capable of reacting with metal cations. The FTIR spectra of L-HA and L-HA-U samples (Fig. 2) revealed the changes in intensity of vibration after the functional groups of L-HA reacted with U(VI) (Garczarek and Gerwert, 2006; Solimannejad and Scheiner, 2008; Mukhopadhyay et al., 2010). The asymmetric COO− stretching frequency shifted from 1353 to 1346 cm^{-1} (a red shift), indicating that U(VI) was adsorbed onto L-HA by COO−. However, the phenolic−OH, —COOH (1700 cm^{-1}) and —OH (3314 cm^{-1}) stretching frequencies had little change, suggesting the lack of reactions of U(VI) with phenolic−OH, —COOH and —OH. Carboxylic and phenolic−OH groups of HA are viewed as the most important metal cation carriers in the formation of metal complexation groups (Bradl, 2014; Tan, 2014). On the basis of the Henderson-Hasselbalch equation, the ionization constant (pK_a) of COOH and phenolic−OH

Table 3
Parameters of kinetic models for U(VI) desorption from L-HA in 1 mM $NaNO_3$ and artificial seawater.

	q_e	Pseudo-first-order			Pseudo-second-order		
		q_1 (mg•g^{-1})	k_1 (1•h^{-1})	R^2	q_2 (mg•g^{-1})	k_2 (g• (mg•h)$^{-1}$)	R^2
1 mM $NaNO_3$	18.7	19.3	0.66	0.97	23.9	0.027	0.95
Artificial seawater	125	122	2.36	0.99	137	0.024	0.99

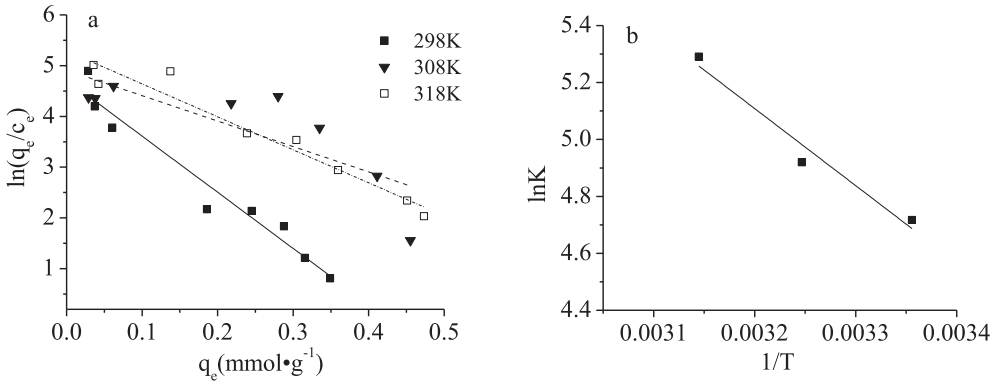

Fig. 7. (a) Plot of ln (q_e/C_e) versus q_e at different temperatures, (b) plot of lnK_0 versus 1/T.

are 3.0 and 10.0, respectively (Tan, 2014). Under the batch isotherm adsorption experiment conditions of this study (pH < 5) the phenolic−OH groups were almost non-ionized. Thus, carboxyl would be the dominant functional groups to adsorb U(VI). Further, a better fitting of U(VI) adsorption data to a pseudo-second-order model, rather than to a pseudo-first-order model, indicates the adsorption process involved chemisorption. Therefore, the main type of chemisorption may be surface complexation of U with the carboxyl groups of L-HA.

4. Conclusions

L-HA produced from leonardite with the traditional alkali-acid method had a high carboxyl ion content and spherical morphology. U(VI) adsorption onto the L-HA was pH-dependent and the time to reach equilibrium was 2 h. The calculated maximum adsorption capacity of L-HA for U(VI) was 91, 112 and 120 mg g^{-1} at 298, 308 and 318 K, respectively. Adsorption data fitted a pseudo-second-order model better than pseudo-first-order model, suggesting the chemisorption nature of U(VI) binding onto L-HA. The adsorption was spontaneous and an endothermic based on thermodynamic data. Desorption of U(VI) from L-HA-U reached equilibrium in 3 h and the percentages of desorbed U(VI) were only 0.06% in simulated soil solution (1 mM $NaNO_3$) and 0.40% in artificial seawater. Addition of L-HA to U-contained wastes may decrease its risks to ecosystem and human health. Being abundant, inexpensive, effective and environmentally friendly, L-HA has a good potential to become a useful adsorbent for use in U- and DU-contaminated sites.

Acknowledgements

This study was supported by the U.S. Army Environmental Quality Technology (EQT) Program, the U.S. Army Engineer Research and Development Center (W912HZ-16-2-0021), the U.S. Nuclear Regulatory Commission (NRC-HQ-84-15-G-0042 and NRC−HQ-12-G-38-0038) and the U.S. Department of Commerce (NA11SEC4810001-003499). FD Meng and GD Yuan acknowledge the support from Chinese National Key Research and Development Program (2016YFD0200303-4) and Key Research and Development Program of Shandong Province (2016CYJS05A01-1). Additionally, we thank personnel from the University of Southern Mississippi, Department of Chemistry and Biochemistry, who provided support for FTIR analyses.

References

Anagnostopoulos, V.A., Katsenovich, Y., Denham, M., 2017. Sodium silicate treatment for the attenuation of U (VI) by iron-bearing sediments in acidic groundwater plumes. J. Chem. Technol. Biot. 92, 1919−1927.
Army Environmental Policy Institute (AEPI), 1995. Health and Environmental Consequences of Depleted Uranium Use in the US Army. Technical Report. US Army Environmental Policy Institute, Atlanta/USA. June 1995.
Anirudhan, T.S., Bringle, C.D., Rijith, S., 2010. Removal of uranium(VI) from aqueous solutions and nuclear industry effluents using humic acid-immobilized zirconium-pillared clay. J. Environ. Radioact. 101, 267−276.
Betti, M., 2003. Civil use of depleted uranium. J. Environ. Radioact. 64, 113−119.
Berthelot, D., Haggis, M., Payne, R., McClarty, D., Courtin, M., 1999. Application of water covers, remote monitoring and data management systems to environmental management at uranium tailings sites in the Serpent River Watershed. Cim. Bull. 92, 70−77.
Biehler, D., Falck, W.E., 1999. Simulation of the effects of geochemical reactions on groundwater quality during planned flooding of the Königstein uranium mine, Saxony. Ger. Hydrogeol. J. 7, 284−293.
Boparai, H.K., Joseph, M., O'Carroll, D.M., 2011. Kinetics and thermodynamics of cadmium ion removal by adsorption onto nano zerovalent iron particles. J. Hazard. Mater 186, 458−465.
Bradl, H.B., 2014. Adsorption of heavy metal ions on soils and soils constituents. J. Colloid Interf. Sci. 277, 1−18.
Camacho, L.M., Deng, S., Parra, R.R., 2010. Uranium removal from groundwater by natural clinoptilolite zeolite: effects of pH and initial feed concentration. J. Hazard. Mater 175, 393−398.
Campos, M.B., de Azevedo, H., Nascimento, M.R.L., Roque, C.V., Rodgher, S., 2011. Environmental assessment of water from a uranium mine (Caldas, Minas Gerais State, Brazil) in a decommissioning operation. Environ. Earth Sci. 62, 857−863.
Campos, B., Aguilar-Carrillo, J., Algarra, M., Gonçalves, M.A., Rodríguez-Castellón, E., da Silva, J.C.G.E., Bobos, I., 2013. Adsorption of uranyl ions on kaolinite, montmorillonite, humic acid and composite clay material. Appl. Clay Sci. 85, 53−63.
Choy, C.C., Korfiatis, G.P., Meng, X., 2006. Removal of depleted uranium from contaminated soils. J. Hazard. Mater 136, 53−60.
Cordfunke, E.H.P., 1970. The Chemistry of Uranium. Elsevier Pub. Co, Amsterdam, New York, p. 21.
Donat, R., 2009. The removal of uranium (VI) from aqueous solutions onto natural sepiolite. J. Chem. Thermodyn. 41, 829−835.
Dulama, M., Iordache, M., Deneanu, N., 2013. Treatment of uranium contaminated wastewater-A review. Nuclear 80−86.
Ellis, A.J., 1963. The effect of temperature on the ionization of hydrofluoric acid. J. Chem. Soc. 4300−4304.
Garczarek, F., Gerwert, K., 2006. Functional waters in intraprotein proton transfer monitored by FTIR difference spectroscopy. Nature 439, 109−112.
Gavrilescu, M., Pavel, L.V., Cretescu, I., 2009. Characterization and remediation of soils contaminated with uranium. J. Hazard. Mater 163, 475−510.
Global Security, 2008. Depleted Uranium (DU) History. Available online: (Accessed 5 2017). www.globalsecurity.org/military/systems/munitions/du-history.htm.
Harter, R.D., Naidu, R., 2001. An assessment of environmental and solution parameter impact on trace-metal sorption by soils. Soil Sci. Soc. Am. J. 65, 597−612.
Havelcová, M., Mizera, J., Sýkorová, I., Pekař, M., 2009. Sorption of metal ions on lignite and the derived humic substances. J. Hazard. Mater 161, 559−564.
Ho, Y.S., 2004. Citation review of Lagergren kinetic rate equation on adsorption reactions. Scientometrics 59, 171−177.
Ho, Y.S., 2006. Review of second-order models for adsorption systems. J. Hazard. Mater 136, 681−689.
Ho, Y.S., McKay, G., 1999. Pseudo-second-order model for sorption processes. Process Biochem. 34, 451−465.
Kalin, M., Wheeler, W.N., Meinrath, G., 2004. The removal of uranium from mining waste water using algal/microbial biomass. J. Environ. Radioact. 78, 151−177.
Khalili, F., Al-Banna, G., 2015. Adsorption of uranium (VI) and thorium (IV) by insolubilized humic acid from Ajloun soil−Jordan. J. Environ. Radioact. 146, 16−26.
Kochany, J., Smith, W., 2001. Application of Humic Substances in Environmental

Remediation. WM'01 Conference.
Konvalinka, J.A., Scholten, J.J.F., Rasser, J.C., 1977. Analysis of second-order desorption kinetics in temperature-programmed desorption. J. Catal. 48, 365–373.
Krestou, A., Panias, D., 2004. Uranium(VI) speciation diagrams in the $UO_2^{2+}/CO_3^{2-}/H_2O$ system at 25°C. Eur. J. Min. Process. Environ. Prot. 4, 113–129.
Krestou, A., Xenidis, A., Panias, D., 2004. Mechanism of aqueous uranium (VI) uptake by hydroxyapatite. Min. Eng. 17, 373–381.
Kütahyalı, C., Eral, M., 2010. Sorption studies of uranium and thorium on activated carbon prepared from olive stones: kinetic and thermodynamic aspects. J. Nucl. Mater 396, 251–256.
Ladshaw, A.P., Das, S., Liao, W.P., Yiacoumi, S., Janke, C.J., Mayes, R.T., Dai, S., Tsouris, C., 2015. Experiments and modeling of uranium uptake by amidoxime-based adsorbent in the presence of other ions in simulated seawater. Ind. Eng. Chem. Res. 55, 4241–4248.
Larson, S.L., Ballard, J., Medina, V., Thompson, M., O'Connor, G., Griggs, C., Nestler, C., 2009. Separation of Depleted Uranium from Soil. ERDC/EL TR-09–1. U. S. Army Engineer Research and Development Center, Vicksburg, MS.
Lasheen, M.R., Ammar, N.S., Ibrahim, H.S., 2012. Adsorption/desorption of Cd (II), Cu (II) and Pb (II) using chemically modified orange peel: equilibrium and kinetic studies. Solid State Sci. 14 (2), 202–210.
Lienert, C., Short, S.A., von Gunten, H.R., 1994. Uranium infiltration from a river to shallow groundwater. Geochim. Cosmochim. Ac 58, 5455–5463.
McKinley, J.P., Zachara, J.M., Heald, S.M., Dohnalkova, A., Newville, M.G., Sutton, S.R., 2004. Microscale distribution of cesium sorbed to biotite and muscovite. Environ. Sci. Technol. 38, 1017–1023.
Meinrath, A., Schneider, P., Meinrath, G., 2003. Uranium ores and depleted uranium in the environment – with a reference to uranium in the biosphere from the Erzgebirge/Sachsen. Ger. J. Environ. Rad. 64, 175–193.
Mellah, A., Chegrouche, S., Barkat, M., 2006. The removal of uranium(VI) from aqueous solutions onto activated carbon: kinetic and thermodynamic investigations. J. Colloid Interf. Sci. 296, 434–441.
Meng, F.D., Yuan, G.D., Wei, J., Bi, D.X., Wang, H.L., Liu, X.Y., 2016. Humic acid from leonardite for Cd adsorption and potential applications. J. Zhejiang Uni. (Agric Life Sci.) 42, 460–468 (in Chinese with English abstract).
Michelsen, H.A., Rettner, C.T., Auerbach, D.J., 1992. On the influence of surface temperature on adsorption and desorption in the D_2/Cu (111) system. Surf. Sci. 272, 65–72.
Milja, T.E., Prathish, K.P., Rao, T.P., 2011. Synthesis of surface imprinted nanospheres for selective removal of uranium from simulants of Sambhar salt lake and ground water. J. Hazard. Mater 188, 384–390.
Misaelides, P., Godelitsas, A., Filippidis, A., Charistos, D., Anousis, I., 1995. Thorium and uranium uptake by natural zeolitic materials. Sci. Total Environ. 173, 237–246.
Mudd, G.M., Patterson, J., 2010. Continuing pollution from the Rum Jungle U–Cu project: a critical evaluation of environmental monitoring and rehabilitation. Environ. Pollut. 158, 1252–1260.
Mukhopadhyay, A., Pandey, P., Chakraborty, T., 2010. Blue-and red-shifting CH··· O hydrogen bonded complexes between haloforms and ethers: correlation of donor νC– H spectral shifts with C– O– C angular strain of the acceptors. J. Phys. Chem. A 114, 5026–5033.
Munasinghe, P.S., Madden, M.E.E., Brooks, S.C., Madden, A.S.E., 2015. Dynamic interplay between uranyl phosphate precipitation, sorption, and phase evolution. Appl. Geochem. 58, 147–160.
Olivella, M.A., del Rio, J.C., Palacios, J., Vairavamurthy, M.A., de las Heras, F.X.C., 2002. Characterization of humic acid from leonardite coal: an integrated study of PY-GC-MS, XPS and XANES techniques. J. Anal. Appl. Phys. 63, 59–68.
Raji, C., Anirudhan, T.S., 1998. Batch Cr(VI) removal by polyacrylamide-grafted sawdust: kinetics and thermodynamics. Water Res. 32, 3772–3780.
Santos, E.A., Ladeira, A.C., 2011. Recovery of uranium from mine waste by leaching with carbonate-based reagents. Environ. Sci. Technol. 45, 3591–3597.
Shaker, M.A., Albishri, H.M., 2014. Dynamics and thermodynamics of toxic metals adsorption onto soil-extracted humic acid. Chemosphere 111, 587–595.
Soler-Rovira, P., Madejón, E., Madejón, P., Plaza, C., 2010. In situ remediation of metal contaminated soils with organic amendments: role of humic acids in copper bioavailability. Chemosphere 79, 844–849.
Solimannejad, M., Scheiner, S., 2008. Complexes pairing hypohalous acids with nitrosyl hydride. Blue shift of a NH bond that is uninvolved in a H-bond. J. Phys. Chem. A 112, 4120–4124.
Steinhauser, G., Brandl, A., Johnson, T.E., 2014. Comparison of the Chernobyl and Fukushima nuclear accidents: a review of the environmental impacts. Sci. Total Environ. 470, 800–817.
Stevenson, F.J., 1994. Humus Chemistry. Genesis, Composition, Reactions, second ed. Wiley, New York.
Tan, K.H., 2014. Humic Matter in Soil and the Environment: Principles and Controversies, second ed. CRC Press, Boca Raton.
Todorov, P.T., Ilieva, E.N., 2006. Contamination with uranium from natural and anthropological sources. Rom. J. Phys. 51, 27–34.
Toque, C., Milodowski, A.E., Baker, A.C., 2014. The corrosion of depleted uranium in terrestrial and marine environments. J. Environ. Radioact. 128, 97–105.
Tsai, S.C., Wang, T.H., Wei, Y.Y., Yeh, W.C., Jan, Y.L., Teng, S.P., 2008. Kinetics of Cs adsorption/desorption on granite by a pseudo first order reaction model. J. Radioanal. Nucl. Ch 275, 555–562.
U.S. Environmental Protection Agency, 2012. Drinking Water Standards and Health Advisories. EPA 822-S-12–1001. Office of Water, U.S. Environmental Protection Agency, Washington, DC.
Uslu, G., Tanyol, M., 2006. Equilibrium and thermodynamic parameters of single and binary mixture biosorption of lead (II) and copper (II) ions onto Pseudomonas putida: effect of temperature. J. Hazard. Mater 135, 87–93.
Van den Boomgaard, T., King, T.A., Tadros, T.F., Vincent, B., 1978. The influence of temperature on the adsorption and adsorbed layer thickness of various molecular weight fractions of poly (vinyl alcohol) on polystyrene latex particles. J. Colloid Interf. Sci. 66, 68–76.
Wang, G., Liu, J., Wang, X., Xie, Z., Deng, N., 2009. Adsorption of uranium (VI) from aqueous solution onto cross-linked chitosan. J. Hazard. Mater 168, 1053–1058.
Wang, J., Hu, X., Liu, Y., Xie, S., Bao, Z., 2010. Biosorption of uranium (VI) by immobilized Aspergillus fumigatus beads. J. Environ. Radioact. 101, 504–508.
World Health Organization, 2008. Guidelines for Drinking-water Quality, third ed.
Xie, S.B., Zhang, C., Zhou, X.H., Yang, J., Zhang, X.J., Wang, J.S., 2009. Removal of uranium (VI) from aqueous solution by adsorption of hematite. J. Environ. Radioact. 100, 162–166.
Yang, C., 1998. Statistical mechanical study on the Freundlich isotherm equation. J. Colloid Interf. Sci. 208, 379–387.
Yang, K., Miao, G.F., Wu, W.H., Lin, D.H., Pan, B., Wu, F.C., Xing, B.S., 2015. Sorption of Cu^{2+} on humic acids sequentially extracted from a sediment. Chemosphere 138, 657–663.
Yu, K., Tan, X., Hu, Y.N., Chen, F.W., Li, S.J., 2011. Microstructure effects on the electrochemical corrosion properties of Mg–4.1% Ga–2.2% Hg alloy as the anode for seawater-activated batteries. Corros. Sci. 53, 2035–2040.
Yuan, G.D., Theng, B.K.G., 2012. Clay-organic interactions in soil environments. In: Huang, P.M., Sumner, M., Li, Y.C. (Eds.), Handbook of Soil Science: Resource Management and Environmental Impacts, second ed. CRC Press, Taylor & Francis Group, Boca Raton. 2–1–2-20.
Ziółkowska, A., 2015. The role of humic substances in detoxification process of the environment. Environ. Prot. Nat. Resou 26, 1–5.

REPORT DOCUMENTATION PAGE

Form Approved
OMB No. 0704-0188

1. REPORT DATE (DD-MM-YYYY)	2. REPORT TYPE	3. DATES COVERED (From - To)
July 2020	Final	

4. TITLE AND SUBTITLE

Removing Uranium (VI) from Aqueous Solution With Insoluble Humic Acid Derived from Leonardite

5a. CONTRACT NUMBER

5b. GRANT NUMBER

5c. PROGRAM ELEMENT NUMBER
633728 03F

6. AUTHOR(S)

Fande Meng, Guodong Yuan, Steven L. Larson, John H. Ballard, Charles A. Waggoner, Zikri Arslan, and Fengxiang X. Han

5d. PROJECT NUMBER
458170

5e. TASK NUMBER
5

5f. WORK UNIT NUMBER

7. PERFORMING ORGANIZATION NAME(S) AND ADDRESS(ES)
U.S. Army Engineer Research and Development Center
Environmental Laboratory
3909 Halls Ferry Road
Vicksburg, MS 39180

8. PERFORMING ORGANIZATION REPORT NUMBER

ERDC/EL MP-20-8

9. SPONSORING / MONITORING AGENCY NAME(S) AND ADDRESS(ES)
Budget and Programs Div
Department of the Army USACE
441 G Street NW
Washington, DC 20314

10. SPONSOR/MONITOR'S ACRONYM(S)

USACE

11. SPONSOR/MONITOR'S REPORT NUMBER(S)

12. DISTRIBUTION / AVAILABILITY STATEMENT
Approved for public release; distribution is unlimited.

13. SUPPLEMENTARY NOTES
Originally published in the Journal of Environmental Radioactivity, September 2017.
Collaborative work was conducted by the U.S. Army ERDC and Jackson State University via Cooperative Agreement W912HZ-16-2-002.

14. ABSTRACT

The occurrence of uranium (U) and depleted uranium (DU)-contaminated wastes from anthropogenic activities is an important environmental problem. Insoluble humic acid derived from leonardite (L-HA) was investigated as a potential adsorbent for immobilizing U in the environment. The effect of initial pH, contact time, U concentration, and temperature on U(VI) adsorption onto L-HA was assessed. The U(VI) adsorption was pH-dependent and achieved equilibrium in 2 h. It could be well described with pseudo-second- order model, indicating that U(VI) adsorption onto L-HA involved chemisorption. The U(VI) adsorption mass increased with increasing temperature with maximum adsorption capacities of 91, 112 and 120 mg g^{-1} at 298, 308 and 318 K, respectively. The adsorption reaction was spontaneous and endothermic. We explored the processes of U(VI) desorption from the L-HA-U complex through batch desorption experiments in 1 mM $NaNO_3$ and in artificial seawater. The desorption process could be well described by pseudo-first-order model and reached equilibrium in 3 h. L-HA possessed a high propensity to adsorb U(VI). Once adsorbed, the release of U(VI) from L-HA-U complex was minimal in both 1 mM $NaNO_3$and artificial seawater (0.06% and 0.40%, respectively). Being abundant, inexpensive, and safe, LHA has good potential for use as a U adsorbent from aqueous solution or immobilizing U in soils.

15. SUBJECT TERMS

Uranium contamination, Depleted uranium, Leonardite, Humic acid, Artificial seawater, Desorption, Soil

16. SECURITY CLASSIFICATION OF:			17. LIMITATION OF ABSTRACT	18. NUMBER OF PAGES	19a. NAME OF RESPONSIBLE PERSON
a. REPORT	b. ABSTRACT	c. THIS PAGE			19b. TELEPHONE NUMBER (include area code)
Unclassified	Unclassified	Unclassified	SAR	12	